

Turbulent round jet control using two steady mini-jets

C. Du ^{1,2}, Y. Zhou ¹ and J. Mi ²

¹ Department of Mechanical Engineering, The Hong Kong Polytechnic University, Hung Hom, Kowloon, Hong Kong

² Department of Energy & Resources Engineering, College of Engineering, Peking University, Beijing, China

Abstract

This study investigates experimentally the near-field characteristics of a turbulent round jet under the disturbance of two steady radial mini-jets injected from opposite sides. The exit Reynolds number (Re) of the jet is 8,000. The flow rate ratio (C_m) of the mini-jets to the main jet varies from 0 to 16.5%. It is found that the centerline velocity decay rate of the main jet is accelerated with increasing C_m until $C_m \approx 12\%$ and then decelerated for a further increase in C_m ; meanwhile, the jet spread rate is highest around $C_m \approx 12\%$ in the plane orthogonal to the mini-jet injection plane, though exhibiting little change in the injection plane. An exploration of connection between the perturbed jet and flow immediately downstream of the impact region of the blowing mini-jets points out that the blowing mini-jets generate a predominant quasi-periodical structure in flow prior to issuing from the nozzle exit. The observation is in contrast to the quasi-steady longitudinal counter-rotating vortex pairs, previously reported at $Re = 1,000 \sim 1,500$. The structure plays an important role in altering the flow structure and subsequently in enhancing the centerline velocity decay rate and jet spread rate in the near field of the perturbed jet.

Introduction

As one of typical basic shear flows, jet is widely seen in engineering, e.g. in aero and automobile engines, burners used in various industries and power plants, water-jet machining, electronic equipment cooling, printing and drying. Naturally, its manipulation or control for mixing enhancement has received a great deal of attention in literature. The active control of jets has potential to achieve flexible and drastic flow modifications. Naturally, many active techniques were proposed and investigated with success to different degrees. The concept to use control jets to enhance jet mixing was proposed by Davis [1] and pursued by a number of investigators for steady blowing control jets [2-3]. This work aims to control the mixing performance of a turbulent jet using two steady side radial mini-jets and to improve our understanding of the underlying physics behind the enhanced mixing performance. The mass flow rate ratio (C_m) of mini-jets to main jet is varied from 0 to 16%. The flow structure is measured using both hotwire and laser-induced fluorescence (LIF) flow visualization techniques. The possible connection between the manipulated jet and initial perturbation is explored.

Experimental Details

Experimental arrangement is schematically shown in Fig 1. The jet apparatus consisted of a diffuser, a cylindrical settling chamber of 114 mm in diameter and a smooth contraction nozzle with a diameter of $d = 20$ mm. The chamber was installed with one layer of honeycomb cells and three layers of fine screens. The contraction nozzle had a contraction ratio of 32.5. The nozzle was extended by a 47-mm-long smooth circular passage of an inner diameter $d = 20$ mm, where two opposing radial

orifices of 0.5 mm in diameter were made at 17 mm upstream of the passage exit for injecting mini-jets. The main jet and the mini-jets received air supply from a compressed air source with a constant pressure of 5 bar gauge pressure. The origin of the coordinate system is chosen at the centre of the circular passage exit (Fig 1a). The (x, y) -plane corresponds to the injection plane of the two mini-jets or the V-plane, and the (x, z) -plane or the H-plane is orthogonal to the V-plane.

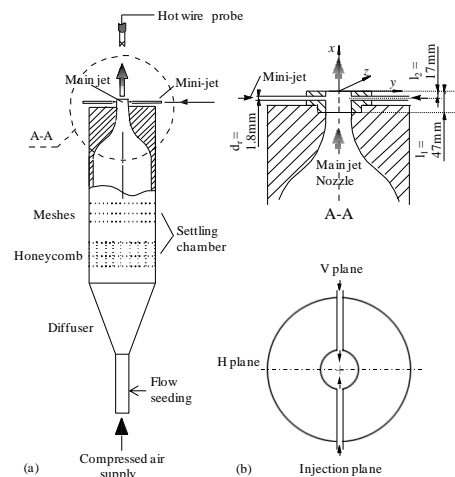


Figure 1. Experimental setup. The V plane is the injection plane of two mini-jets and the H plane is orthogonal to the injection plane.

Experiments were performed at the bulk exit velocity $U_e = 6$ m/sec, corresponding to an exit Reynolds number $Re (\equiv U_e d / \nu)$ of 8,000. Both hotwire and LIF measurements indicated that the round jet was turbulent in the developed region. The C_m was varied from 0% to 16.5%. One single hotwire was used to measure the velocities along the y - and the z -axis (Fig 1b), respectively. The sensing element was made of a $5 \mu\text{m}$ tungsten wire of about 2 mm in length. The hotwire was operated on a constant temperature circuit at an overheat ratio of 1.5. The signal from the single wire was offset, low-pass filtered at a cut-off frequency of 0.92 kHz, and then sampled at a frequency of 1.84 kHz. The sampling duration for each record was 37 s. The hotwire was calibrated in the potential core of the free main jet, using a Pitot-static tube connected to an electronic micro-manometer (Furness FCO510). The hotwire probe was mounted on a 2-D traversing system, with a resolution of 0.1 mm longitudinally and 0.01 mm laterally. The x/d range examined was $0 \sim 30$. One X-wire was also used in order to obtain power spectral density functions, E_u and E_v , of the longitudinal and radial fluctuating velocities, u and v , in both H- and V-planes. The sensors of the X-wire were made of $5 \mu\text{m}$ tungsten wire of approximate 3 mm in length, operated on constant temperature circuits at an overheat ratio of 1.5. The X-wire was calibrated in terms of the effective yaw angle and velocity. The signals from

the X-wire were offset, low-pass filtered at a cut-off frequency of 0.9 kHz, and then sampled at a frequency of 1.8 kHz. The sampling duration was 10s for each record.

The LIF flow visualization was conducted in the (x, y)- and the (x, z)-planes (Fig.1b), using a 2D DANTEC particle image velocimetry system. Flow was seeded with oil droplets of 1 μm in diameter, released from the settling chamber (Fig. 1a). Please refer to reference [35] for more details of the technique and instrumentation. A total of 60 images were captured in each plane.

Results and Discussions

Figure 2 shows the downstream variation of the centreline mean velocity ratio $U_{e,c}/U_c$ for the main jet controlled by the two steady mini-jets for $C_m = 6.4\% \sim 16.5\%$, where U_c is the centreline mean velocity. The data of the free main jets presently measured at $Re = 8,000$ and reported in Mi et al. [4] ($Re \approx 1.5 \times 10^4$) and Quinn [5] ($Re = 2.0 \times 10^5$) are also presented. As noted immediately, the ratio $U_{e,c}/U_c$ exhibits an approximately linear variation for $x/d > 5$. That is, the centreline velocity decay of the free jets conforms to the self-preservation relationship $U_{e,c}/U_c = K \cdot (x - x_0)/d$, where x_0 is the streamwise position of the virtual origin and slope K provides a measure for the velocity decay rate. The present data of the uncontrolled jet exhibit an approximately parallel shift from those of Mi et al. and Quinn. The present $U_{e,c}/U_c$ is highest and Quinn's measurement is lowest. The deviation between the three measurements appears mainly ascribed to the Reynolds number effect on the centreline velocity decay rate. The explanation is fully consistent with Malmstrom et al.'s observation that the decay rate of the normalized centreline velocity decreased as Re increased until a critical value was reached [5].

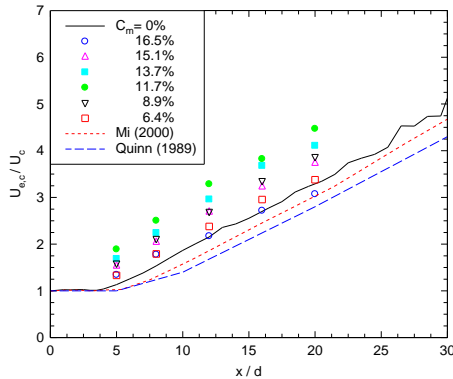


Figure 2 Dependence of the centreline velocity ratio $U_{e,c}/U_c$ on the mass ratio (C_m) of the mini-jets to the main jet.

It is evident in Figure 2 that, as C_m is increased, the ratio $U_{e,c}/U_c$ rises until $C_m = 11.7\%$ and then falls for a further increase in C_m . This implies that the higher C_m leads to the larger entrainment rate for $C_m < 11.7\%$ but produces the opposite effect for $C_m > 11.7\%$. The observation is valid in the near field ($x/d \leq 5$), not further downstream. This point is made evident by the dependence of $\Delta U/U_e$ on C_m in Figure 3, where $\Delta U_1 = U_e - U_{x=5d}$ and $\Delta U_2 = U_{x=15d} - U_{x=20d}$ with $U_{x=5d}$, $U_{x=15d}$ and $U_{x=20d}$ being the centreline mean velocity at $x/d = 5, 15$ and 20 , respectively. The C_m dependence of the near-field velocity decay rate $\Delta U_1/U_e$ is distinct from that of $\Delta U_2/U_e$ from $x/d = 15$ to 20 . As C_m is increased, $\Delta U_1/U_e$ in the near field grows significantly until $C_m = 11.7\%$ and then retreats. On the other hand, $\Delta U_2/U_e$ does not change much with C_m . In fact, given $x/d > 5$, the minijet control has little effect on the velocity decay rate, that is, the controlled jet recovers its natural decay rate rapidly. The observation re-confirms the previous report [3] that the effect of mini-jet control was efficient only in the vicinity of perturbation.

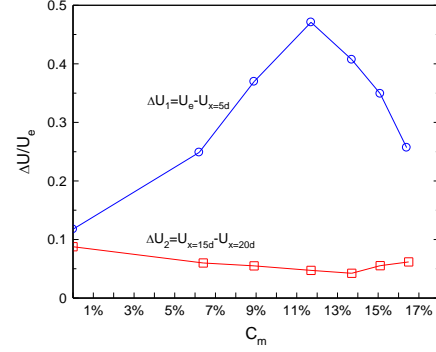


Figure 3 Dependence of $\Delta U/U_e$ on C_m for $Re = 8000$. $U_{x=5d}$, $U_{x=15d}$ and $U_{x=20d}$ are the centreline mean velocity at $x/d = 5, 15$ and 20 , respectively.

Figure 4 shows the dependence on x/d of the mean-velocity half-widths, R_H and R_V , in the H and V planes and the equivalent half-radius $R_{eq} = [R_H R_V]^{1/2}$, which indicates the overall spread of the jet. The half width is defined as the radial distance between the jet axis and the location at which the mean velocity is one half of the centreline mean velocity, and is presently determined from the hotwire-measured radial velocity distributions (not shown) in the two orthogonal planes. Quinn's hot-wire measurement [5] is also included in Figure 4(c) for the purpose of comparison. Note that the free-jet spread rate reported in Ref [5] for $Re = 2 \times 10^5$ is significantly lower than the present data at $Re = 8 \times 10^3$, consistent with the centreline velocity decay rate (Fig 2). The difference reflects the Re dependence of the entrainment rate of a turbulent jet, that is, the entrainment rate decreases with increasing Re . Once the mini-jets are operated, R_H (Fig 4a) grows considerably for the x/d range examined, while the variation in R_V (Fig 4b) is small. That is, the mini-jets' perturbation changes little the spread rate of the main jet in the injection plane but accelerates substantially the spread rate in the plane perpendicular to the injection direction. The observation is corroborated by examining the typical flow structures of the free and controlled jets ($C_m = 11.7\%$) captured by LIF flow visualization. Apparently, the controlled jet is significantly broader in the H plane (Fig 5b) than the free jet (Fig 5a), but not in the V plane (Fig 5c). The above observations agree qualitatively with those of New & Tay [31]. Another observation made from Figure 4 is that the growth in R_H with increasing C_m reaches the maximum at $C_m = 11.7\%$ and a further increased C_m yields a contracted R_H , internally consistent with the observation from the centreline velocity decay rate.

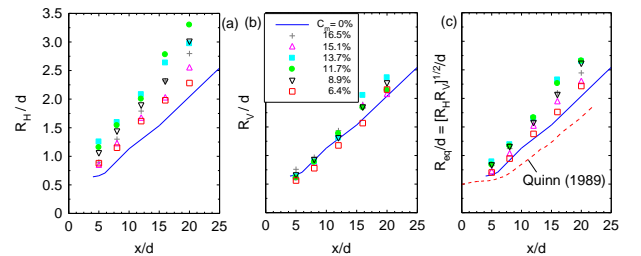


Figure 4 The mean-velocity half-widths. (a) R_H , in the H plane; (b) R_V , in the V plane; and (c) $R = [R_H R_V]^{1/2}$, the equivalent half-radius.

It is of fundamental importance to understand the variations in the velocity decay and spread rates with C_m shown in Figs. 2-4. In the free jet, the circular shear layer appears to roll up and form axisymmetric ring-like laminar vortices very near the nozzle exit ($x/d < 4$) and these structures are then advected downstream (Fig. 5a). The vortices become turbulent or break down from $x/d \approx 4$. Correspondingly, a pronounced peak occurs at the Strouhal number of 0.35 in the power spectra of the centreline u and v measured at $x/d = 3$ (see Fig. 1). With the mini-jets blowing, the underlying flow structure becomes rather distinct. In the V plane,

the mini-jet injection, upstream of the jet exit, may destroy the well-defined shear layer, thus preventing the generation of azimuthal ring vortices. New and Tay [2] observed two pairs of small counter-rotating streamwise vortices in a round jet of $Re = 1,000$ under the perturbation of two radial blowing mini-jets. It is difficult to confirm the presence of such vortices in the present round jet of a much higher Re . The flow structure appears very incoherent, and the coherent structures that are evident in Fig 5a are invisible in the V plane of the controlled jet (Fig. 5c). On the other hand, in the H plane, the less disturbed shear-layer can still roll up, forming the azimuthal vortices. These vortices are more turbulent than those in the free jet and are still identifiable in the near field of the H plane (Fig. 5b), albeit not so symmetrical about the centreline as in the free jet.

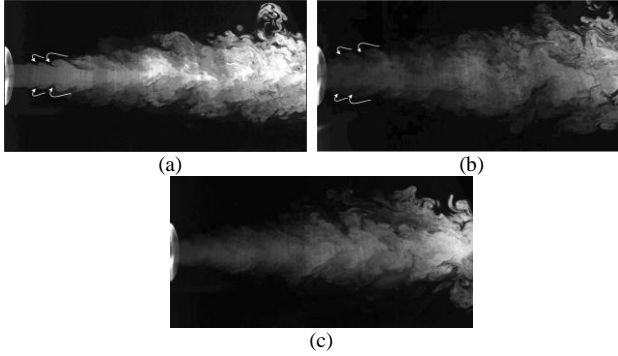


Figure 5 Typical photographs of flow visualization ($x/d \approx 0 - 10$): (a) $C_m = 0$ (without control); (b) $C_m = 11.7\%$, taken in the H plane; (c) $C_m = 11.7\%$, taken in the V plane.

The power spectral density function, E_v , of v measured at $x/d = 1 \sim 6$ and various r/d is examined with and without control in order to gain a better picture of the flow structure alteration. The same scale has been used for ordinate in all the spectra of the free jet (Fig 6) to facilitate comparison and discussion. For the same token, the same scale, which is different from that in Fig 6, is adopted for those under the mini-jet control (Figs 7 & 8). In the free jet (Fig 6), E_v at $x/d = 1$ displays a pronounced peak at $f^* = 0.67$ across the jet. However, at $x/d = 2$, the most prominent peak in E_v occurs at $f^* = 0.35$, with its second harmonic also discernible at $f^* = 0.70$. The peak at $f^* = 0.35$ is even more pronounced at $x/d = 3$ but becomes almost invisible at $x/d = 6$. The pronounced peak in E_v at $x/d = 1$ is probably due to the Kelvin-Helmholtz instability in the shear layer, while that at $x/d = 2 \sim 3$ results from the natural quasi-periodic ring vortices (Fig 5a), which may have broken up when reaching $x/d = 6$. Once the mini-jets are injected, there is a marked change in E_v . The peak seen at $x/d = 1$ in the free jet disappears in the injection V plane (Fig 7a), and the ring vortex at $St = 0.35$ observed at $x/d = 2 \sim 3$ could not be identified either. On the other hand, a peak at $f^* = 0.67$ is still discernible at $x/d = 1$ in the H plane for $r/d \geq 0.5$ (Fig 8a). So is the peak at $St = 0.35$ at $x/d = 2$ (Fig 8b). Nevertheless, the peaks are much more broadened and less pronounced, as a result of the mini-jet perturbation, than in the free jet. Beyond $x/d = 2$ (Fig 8c & d), the peak could not be identified at $St = 0.35$, suggesting that the remnant of the ring vortex vanishes in the perturbed jet more rapidly than in the free jet. The spectral data shown above is essentially consistent with the flow visualization results (Fig 5). Note that the peak in E_v is shifted progressively towards lower frequency for larger r/d , exceeding 0.4 say at $x/d = 2$, or for increasing x/d because of increasing shear layer thickness.

To understand any possible connection of the above observations to the initial perturbation of the mini-jets, a single hot-wire was deployed to measure u at $x/d = -0.7$ and $r/d = 0.35$, almost immediately downstream of the radial mini-jets located at $x/d = -0.85$. In the absence of blowing mini-jets, E_u (Fig 9) exhibits a

number of pronounced peaks due to the resonance in the nozzle cavity (see, e.g., Gutmark et al [7]). Once the mini-jets are operated, a single pronounced peak occurs at $f^* \approx 0.28$ in E_u . Evidently, the mini-jet injection produces a predominant quasi-periodic coherent structure in the flow prior to its issue from the nozzle exit. As a matter of fact, a peak at $f^* \approx 0.28$ is still discernible at $x/d = 1$ in the injection V plane. Please refer to the spectra measured at $r/d = 0.6 \sim 0.8$ in Fig 7a.

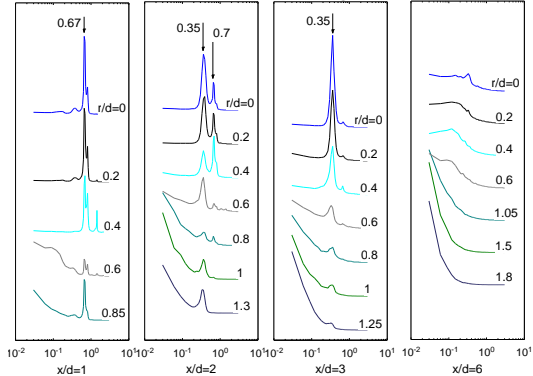


Figure 6 Power spectral density function, E_v , of the centreline v measured at various r/d in the free jet ($C_m = 0$). $Re = 8,000$.

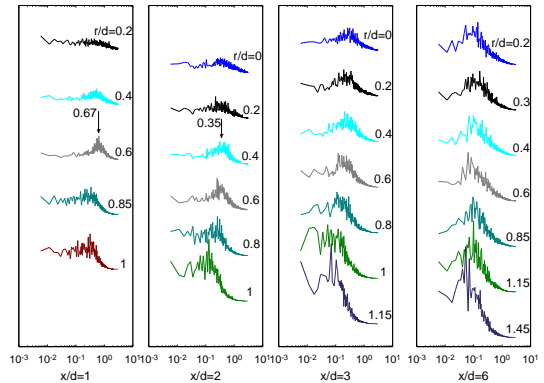


Figure 7 Power spectral density function, E_v , of the centreline v measured at various r/d in the H plane of the controlled jet. $Re = 8000$, $C_m = 11.3\%$.

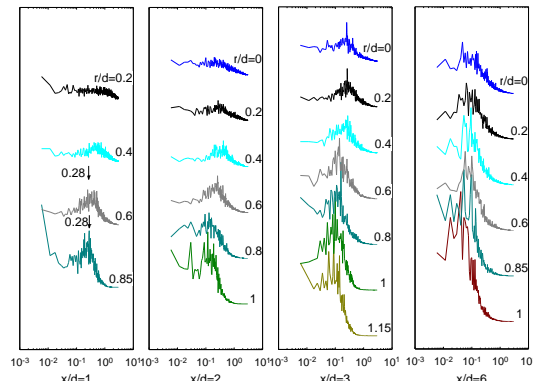


Figure 8 Power spectral density function, E_v , of the centreline v measured at various r/d in the V plane of the controlled jet. $Re = 8000$, $C_m = 11.7\%$.

There is no such peak in the H plane or beyond $x/d = 1$ (Fig 7). Lardeau et al. [2] performed the direct numerical simulation (DNS) of a round jet ($Re = 1,500$) perturbed by two axisymmetric control jets. The control jets were inclined with respect to the streamwise direction of the main jet and their mass flux was near 20% of the main jet mass flux. Two pairs of quasi-steady longitudinal counter-rotating vortices were observed downstream of the impact region of the control jets. Each pair was associated with the impact of one control jet. A similar observation was made experimentally at $Re = 1,000$ when two radial mini-jets

were deployed. In the context of the present relatively high Reynolds number ($Re = 8,000$), it is difficult to capture the longitudinal counter-rotating vortices, if any. The quasi-periodical coherent structures, indicated in Fig 9, are apparently not the same as the quasi-steady longitudinal structures [2-3]. The difference is probably attributed to a disparity in the Reynolds numbers of both the main jet and control jets; it further suggests that the flow structure of the mini-jet perturbed jet be distinct at a high Re from that at a low Re .

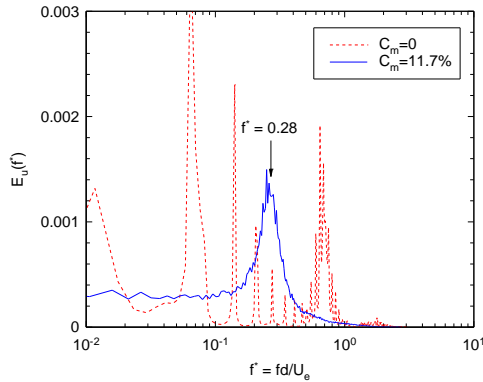


Figure 9 Power spectral density function of a hot-wire signal u obtained at $x/d = -0.7$ and $r/d = 0.35$ in the V plane, downstream of the mini-jets, for $Re = 8,000$.

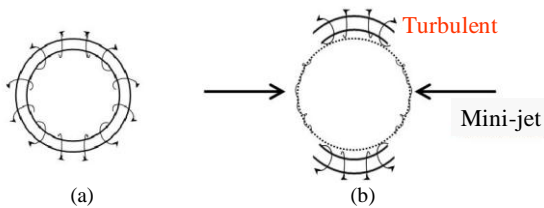


Figure 10 (a) Axisymmetric ring vortex in a free jet, (b) altered flow structure with mini-jets blowing.

A scenario is now proposed for the development of the mini-jet-controlled jet. The two radial blowing mini-jets produce quasi-periodical coherent structures of a dimensionless frequency of $f^* = 0.28$ under present experimental conditions. The structures alter flow separation from the nozzle. The shear layer rollup is suppressed and no vortices could be seen about the injection plane (Figs 5c & 7). On the other hand, the shear layer rollup remains discernible about the plane orthogonal to the injection plane (Fig 5b), forming vortical structures, albeit weak in strength (Fig 8a-b). The remnant of the ring vortex is now fully turbulent. As such, the laminar ring vortex in the free jet (Fig 10a) is replaced by turbulent non-axisymmetric structures (Fig 10b). Two factors may contribute to the accelerated velocity decay rate with mini-jets blowing. Firstly, the loss of axisymmetry by coherent structures may accelerate the velocity decay [1]. Azimuthal non-uniformities at the jet exit may enhance greatly not only large-scale but also small-scale mixing as a result of amplified high azimuthal instability modes [1]. Secondly, being turbulent, the vortical structures may entrain more free-stream fluid into the jet and enhance significantly mixing about the H-plane, resulting in enlarged R_H/d (Fig 4a), though the absence of vortices near the V or injection plane leads to almost unchanged R_V/d (Fig 4b). The resultant effect is an enhanced velocity decay rate (Fig 2) and jet mixing (Fig 4c). The effect of the blowing mini-jets on the velocity decay rate and jet mixing is marked only in the near field ($x/d < 5$) of the main jet (Fig 3), and the jet recovers its natural decay rate rapidly (Fig 2). On the other hand, the blowing-mini-jet-produced structures persist only up to $x/d \approx 1$ (Fig 7). A possible connection between the two observations could not be excluded. Beyond a certain level of C_m , the blowing mini-jets are so strong that the turbulent vortex rollup in the H

plane would be weakened and even suppressed, as in the V plane. As a result, $\Delta U/U_e$ retreats (Fig 3).

Conclusions

This study investigated at a fixed Reynolds number the active control of a turbulent round jet using two steady radial blowing mini-jets. The mass ratio C_m examined was from 0% to 16.5%. The hotwire and LIF flow visualization data with control was carefully analysed and compared with that without control. Following conclusions may be drawn out of the investigation.

It has been found that the blowing mini-jets produce quasi-periodical structures prior to the issue of flow from the nozzle exit, in distinct contrast to the quasi-steady longitudinal counter-rotating vortex pairs, previously observed at $Re = 1,000$ -1,500 [31-32]. The difference is ascribed to the present higher Reynolds numbers of both the main and control jets. The occurrence of these structures alters the way the ring vortex separates, as schematically shown in Fig 10 and subsequently the main jet decay and spread rates. These structures are short-lived after issuing from the nozzle exit, which may well explain why the effect of the mini-jets on jet mixing is limited to the near field of the main jet and the perturbed jet recovers its natural decay rate after $x/d = 5$.

For a given configuration of continuously blowing mini-jets, the jet spread rate grows with increasing C_m , as expected, but retracts after reaching a maximum. Two factors are responsible for the growth. Firstly, the mini-jet injection results in the loss of axisymmetry in vortices generated. The coherent structures cannot be observed in the injection or V plane but persist about the orthogonal H plane. Accordingly, the mean velocity half width in the H plane exceeds about 50% of that in the V plane or in the plain jet. Secondly, the interaction between the mini-jets and the main jet leads to a transition of the laminar vortices to the turbulent in the near field of the jet, which enhances entrainment and mixing. It is proposed that a further increase in C_m beyond that achieving the maximum jet spread rate may act to weaken the turbulent vortices, thus resulting in the observed drop in the jet spread rate.

Acknowledgments

YZ wishes to acknowledge support given to him from Research Grants Council of HKSAR through grant PolyU 5334/06E and from The Hong Kong Polytechnic University through grant G-U507.

References

- [1] Davis M R 1982 Variable control of jet decay, *AIAA Journal*, **20**, 606.
- [2] Lardeau S, Lamballais E & Bonnet J-P 2002 Direct numerical simulation of a jet controlled by fluid injection, *Journal of Turbulence*, **3**, 1-25.
- [3] New T H & Tay W L 2006 Effects of cross-stream radial injections on a round jet, *Journal of Turbulence*, **7**, 1-20.
- [4] Mi J, Nathan G J & Luxton R E 2000 Centreline mixing characteristics of jets from nine differently shaped nozzle, *Experiments in Fluids*, **28**, 93-94.
- [5] Quinn WR 1989 Effects of nonparallel exit flow on round turbulent free jets. *Int J Heat & Fluid Flow* **10**: 139-145.
- [6] Malmström TG; Kirkpatrick AT; Christensen B; Knappmiller KD 1997 Centreline velocity decay measurements in low-velocity axisymmetric jets. *J Fluid Mech* **346**: 363-377.
- [7] Gutmark, E., Ho, C.-M. 1983 Preferred Modes and the Spreading Rates of Jets. *Phys. Fl.* **26**: 2932-2938.